Microsc. Microanal. Microstruct. 7 (1996) 161–174 JUNE **1996**, PAGE 161

Classification
Physics Abstracts
61.16.Bg — 68.35.Dv — 68.65+g

Spatially Resolved EELS Fine Structures at a SiO_2/TiO_2 Interface

Nathalie Brun ([1]), Christian Colliex ([1]), Josette Rivory ([2]) and Kui Yu-Zhang ([3])

([1]) Laboratoire de Physique des Solides, URA CNRS 002, Université Paris-Sud, Bât. 510, 91405 Orsay Cedex, France
([2]) Laboratoire d'Optique des Solides, URA CNRS 781, Université P. et M. Curie, 4 Place Jussieu, Tour 13-12, 75252 Paris Cedex 05, France
([3]) Laboratoire de Reconnaissance des Matériaux dans leur Environnement, Université Marne-la-Vallée, 2 rue de la Butte Verte, 93166 Noisy-le-Grand Cedex, France

(Received June 4; accepted September 5, 1996)

Abstract. — SiO_2/TiO_2 multilayers stacks used in optical coatings have been studied by Electron Energy Loss Spectroscopy (EELS). The line-spectrum mode has been used: the incident electron probe of the STEM is scanned under digital control on the specimen surface in the direction perpendicular to the layers, while the whole spectrum is acquired. The selected energy range contains Ti L_{23} and O K edges, in order to study the evolution of the fine structures visible on these edges. Every experimental spectrum is then fitted with a linear combination of the two reference spectra (TiO_2 and SiO_2) extracted from the same sequence. It is possible to identify in the neighbourhood of the interface some EELS fine structures which cannot be fitted to a combination of reference spectra, but are representative of hybrid environments, such as Si-O-Ti in the present study. A quantitative analysis of the changes in different fine structures on the titanium and oxygen edges enables to clearly discriminate different levels of interdiffusion at the boundary.

1. Introduction

SiO_2/TiO_2 multilayers are used in numerous optical coatings for specific applications like antireflection coatings, dielectric mirrors, *etc.* The knowledge of the microstructure of each layer, which affects the value of its refractive index, and of the sharpness of interfaces is necessary for monitoring the deposition process, understanding and controlling the stability of the final product. Optical techniques, such as photometry or ellipsometry have to be corroborated by techniques giving information on the atomic structure and on the local chemical environment of a given species.

Electron Energy Loss Spectroscopy (EELS) combined with High Resolution Transmission Electron Microscopy (HRTEM) has proved to be useful for characterizing the interface SiO_2/TiO_2 in multilayers stacks consisting of very thin layers (a few nanometers) entering in the production of antireflection coatings for eye glasses [1]. However, because in this case the interfaces were

very close to each other, it was difficult to define the reference spectra which are necessary for interpreting correctly the evolution of the EELS spectra across the interfaces. In consequence, we have performed a new study of a SiO_2/TiO_2 stack consisting of thicker layers, analysed with an electron probe of small diameter (0.7 nm). The present work therefore emphasizes new methods for processing quantitatively such spectral sequences in order to investigate the local changes in chemistry and electronic properties across an interface.

2. Materials and Methods

The samples have been prepared in a UHV chamber prepumped down to a pressure of 10^{-8} Torr realized by a combination of turbomolecular and ionic pump. The evaporation is made from two electron beam guns in presence of an oxygen partial pressure of 1.5×10^{-4} Torr. The initial material is Ti_3O_5 with a low proportion of Ti_4O_7 (Optron Inc. 0550). The substrates, which are Si wafers covered of a 140 nm thick thermal SiO_2 layer, were held at 250 °C during deposition. The multilayer stack under study consists of 12 layers. The SiO_2 evaporated layers are about 170 nm thick, the TiO_2 layers are 70 nm thick. Figure 1 shows a scheme of the layer growth sequence.

For HRTEM and EELS investigations, cross-sectional specimens have been prepared by mechanical polishing up to electron transparency by the tripode method. The thinning was completed by ion milling for 10 mn. Microstructural observations have been performed using a Topcon 002B transmission electron microscope (200 kV, $C_s = 1$ mm) and the EELS measurements with a VG HB 501 Scanning Transmission Electron Microscope (STEM) operating at 100 kV and equipped with a parallel detection electron energy loss spectrometer (PEELS 666 Gatan).

In order to connect the spectroscopic information carried by the EELS analysis and its localization with respect to the multilayer sequence, the image-spectrum mode has been used [2]. The incident electron probe of the STEM is scanned under digital control on the specimen surface in the direction perpendicular to the layers, while the whole spectrum over a selected energy range is acquired. The incident beam semi-angle on the sample was 7 mrad, providing an incident probe diameter of about 0.7 nm, and the spectrometer collection semi-angle was 16 mrad. For probing EELS fine structures, acquisition time was 8 s per spectrum, giving a total time of about 9 mn for the 64 spectra. According to chosen magnification, the distance between successive probe positions was 0.6 nm for interface A and 1.2 nm for interface B.

3. Experimental Results

TEM results show that as expected SiO_2 is amorphous, whereas TiO_2 is partially crystalline and exhibits the columnar structure usually found in evaporated films [3]. At this magnification all interfaces appear to be well defined, even after deposition of the 8^{th} layer. But when examining these interfaces at higher magnification, it seems (Fig. 2) that the interface SiO_2/TiO_2 is sharper than the interface TiO_2/SiO_2, because of the emergence of the TiO_2 layer columns into the SiO_2 one (Fig. 2a corresponds to the interface between the first SiO_2 layer and the second TiO_2 layer, Fig. 2b to the interface between the second TiO_2 layer and the third SiO_2 layer). Moreover, Figure 2b shows (111) lattice fringes in the TiO_2 layer corresponding to anatase structure.

It is known that SiO_2 thermal oxides and evaporated films (which are porous) present differences: in the value of their refractive index in the visible, in the frequency of the dominant IR-active bond stretching vibration; this later varies according to the mean value of the bonding angle Si-O-Si between two tetrahedral SiO_4 and depends strongly on the deposition parameters [4, 5]. Ellipsometry measurements have been performed during deposition, at a single wavelength (450 nm), and after deposition of each layer in the spectral range 400-800 nm. Although the

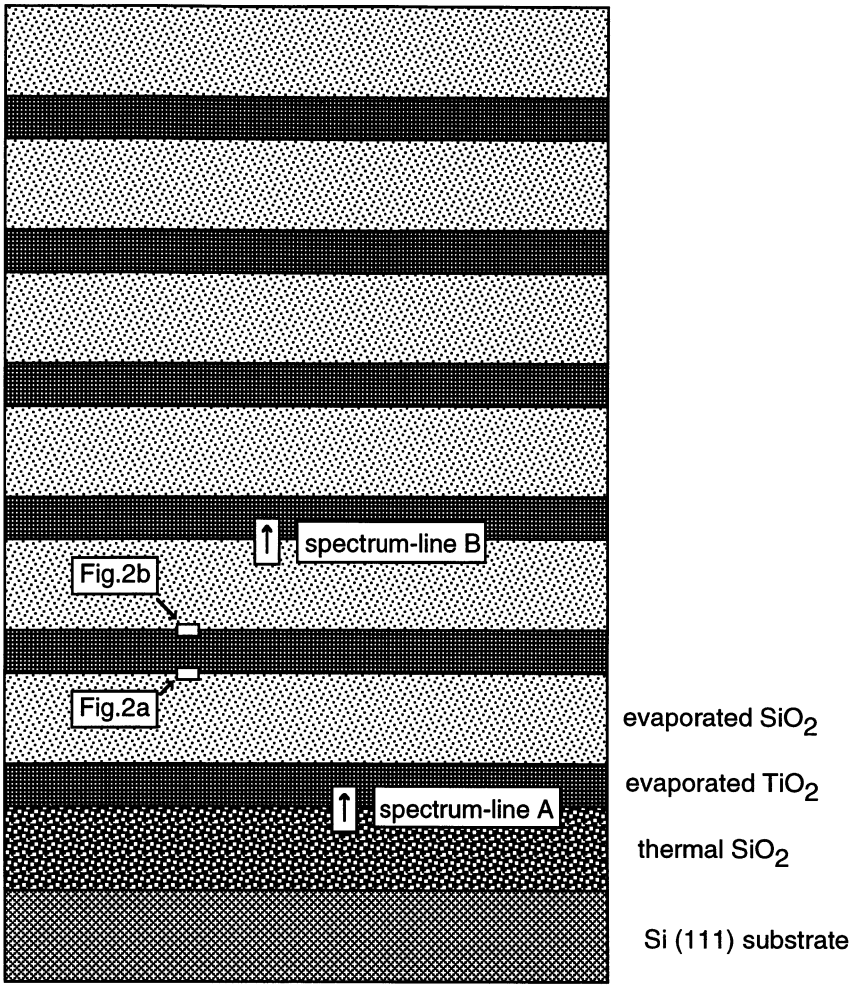

Fig. 1. — Scheme of the SiO_2/TiO_2 stack deposited on a Si wafer covered with a thermal SiO_2 layer.

complete set of results will be reported elsewhere [6], these measurements show that TiO_2 layers grown on thermal SiO_2 have a larger refractive index than on evaporated SiO_2 [7]. For these reasons, it is interesting to compare two types of interfaces:

- A: thermal SiO_2/first TiO_2 layer;
- B: evaporated SiO_2 (second layer)/ third TiO_2 layer.

Spectrum-lines acquired in the low loss region have shown that local sample thickness parallel to the electron beam in the area of interface A is about 125 nm; in the area of interface B, the sample is a wedge with thickness decreasing from about 70 nm (SiO_2 side) to 40 nm (TiO_2 side).

Electron energy loss spectra cover a wide range of electron excitations, from the low energy loss domain involving plasmons and interband transitions to the high energy loss domain exhibiting transitions from different core edges (either Si edges, L_{23} at 100 eV and K at 1850 eV , or Ti edges, M_{23} at 50 eV and L_{23} at 450 eV, or O edge, K at 530 eV). In the present case, we have selected a well defined energy loss range, 200 eV wide, including the characteristic Ti L_{23} and O K edges, in

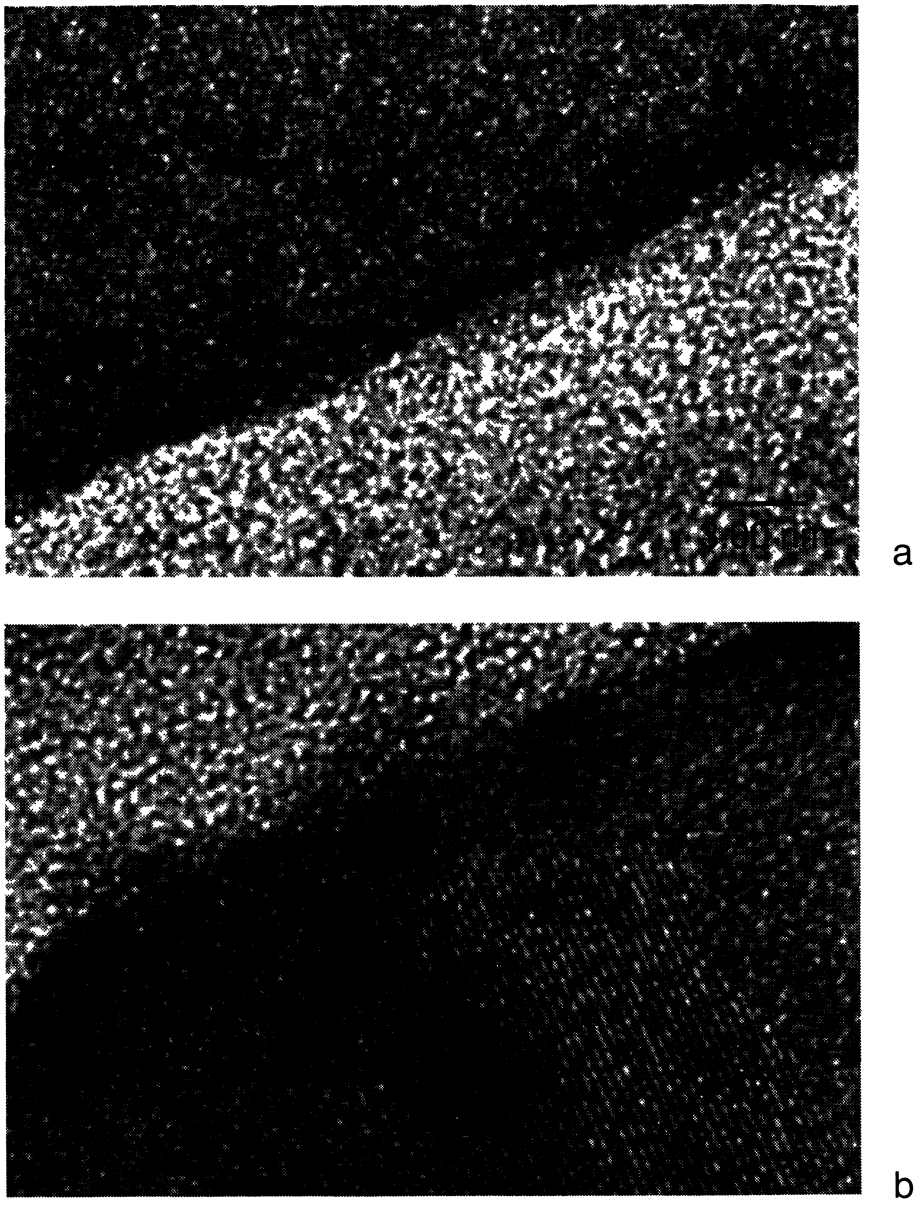

Fig. 2. — HREM image of the SiO_2/TiO_2 interface (a), the TiO_2/SiO_2 interface (b) for the second TiO_2 layer. Lattice fringes correspond to (111) planes of anatase.

order to study the evolution of the fine structures visible on these edges: in fact, each spectrum is made of 1024 channels of 0.2 eV width each. When investigating the detailed chemistry and electron states features across an interface, the most important information lies in the variation between successive spectra corresponding to different positions of the probe.

Figure 3 shows the whole set of data acquired in a spectrum-line made of 64 spectra collected across interface A, and clearly displays changes such as the disappearance of the Ti line when

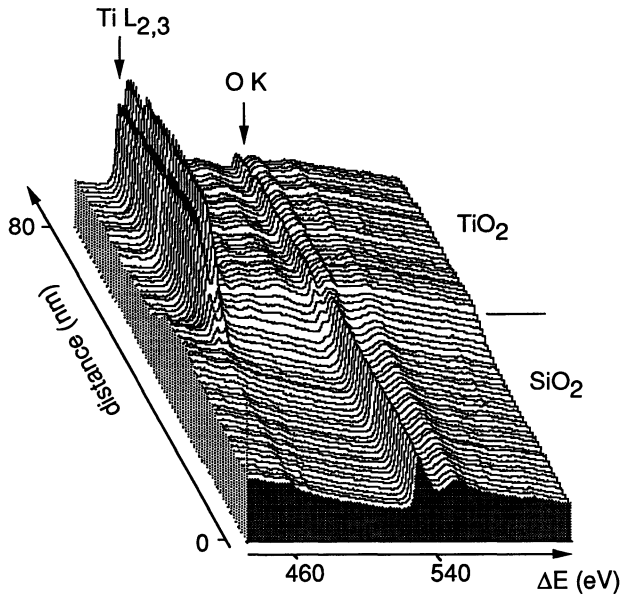

Fig. 3. — 3D representation of a series of EELS spectra recorded while scanning the beam through the interface A. The Ti $L_{2,3}$ edge (455-470 eV) and O K edge (535-550 eV) are recorded.

moving from TiO_2 to SiO_2, and the associated evolution of the shape of the O edge present on both sides of the interface. The next step is to identify and measure these changes. In order to achieve it, it is first necessary to define the reference spectra for the two types of matrix. This is made by adding six successive spectra recorded far from the interface on each side of it: Figure 4 is the reference spectrum for the TiO_2 species in this sequence encompassing both Ti and O contributions, while Figure 5 compares more accurately the fine structures appearing on the O K edge, after background subtraction for the two matrix and the two interfaces. On the TiO_2 side, the Ti $L_{2,3}$ edge exhibits two intense white lines labeled L_3 and L_2 corresponding to the strong transitions from the spin-orbit split levels $2p_{3/2}$ and $2p_{1/2}$ towards unoccupied 3d states close to the Fermi level. Each of these white lines is further split into two components, as a consequence of the crystal field splitting into t_{2g} and e_g type orbitals imposed by the local octahedral symmetry on the Ti ion as well in the anatase as in the rutile structure. At higher energies this edge exhibits a plateau, the intensity of which is modulated by extended fine structures with three peaks labelled (B, C, D). As for the O K edge which is present on both sides of the interface, its fine structure changes significantly when the probe is scanned across the interface. For both investigated interfaces, the O K edge on the SiO_2 side remains similar with an inflexion point at 536 eV and a single broad peak at 538.5 eV. On the titanium side, a strong contribution at lower energy, *i.e.* a kind of doublet prepeak, shifts the inflexion point down to 529 eV, and the energy range between 535 and 545 eV displays variable oscillating fine structures. It has been shown in several XAS or EELS studies on different transition metal oxides [8, 9] that the prepeak corresponds to unoccupied hybridized O 2p-Ti 3d states, and reflects the existence of Ti-O (anti)bonding states. In the previous study concerning the TiO_2-SiO_2 multilayers [1], it has been shown that the presence of this prepeak on the O K edge is very well correlated with the presence of the Ti L edge, confirming the present interpretation.

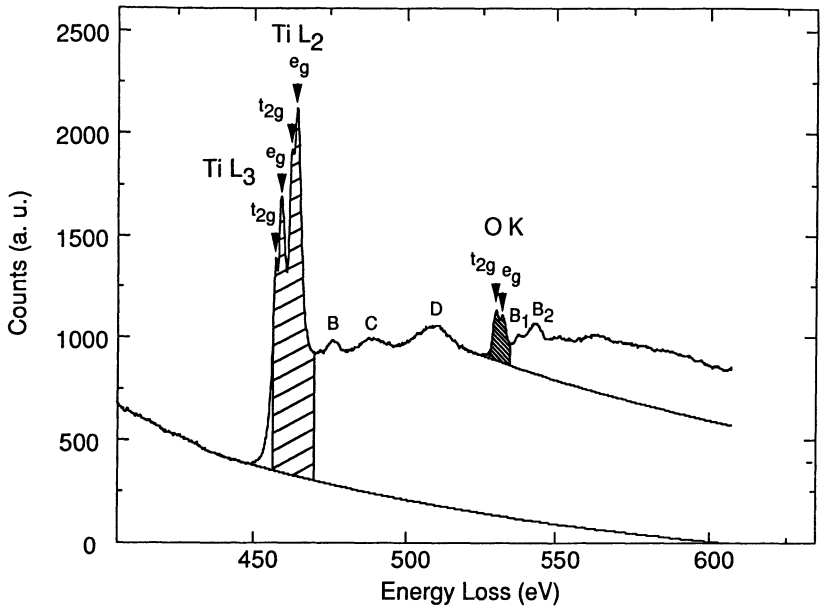

Fig. 4. — Sum of six spectra taken far away of the interface A (spectra 50 to 55) in the TiO_2 part. "Crystal field" splitting is observed on the Ti $L_{2,3}$ edge white lines as well as on the O K edge.

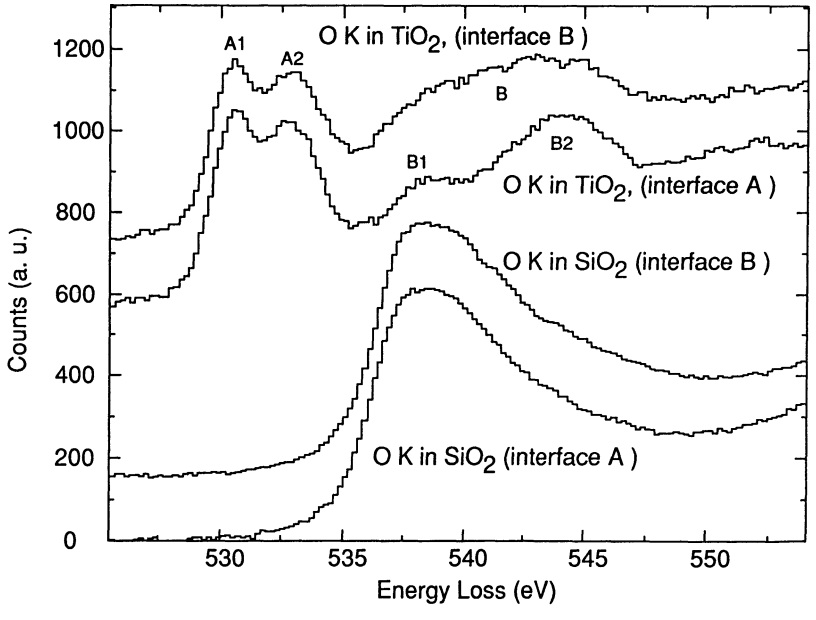

Fig. 5. — O K edge reference spectra obtained as the sum of six spectra taken far from the interfaces: in the SiO_2 part (spectra n°5 to 10), in the TiO_2 part (spectra n°50 to 55).

Above the prepeak (A1, A2), the O K edge in TiO_2 exhibits structures labeled B (extending over 7 or 8 eV) or B1, B2 (clearly separated) which must be attributed to different types of microstructures. The comparison with EELS or X-ray absorption data on rutile and anatase [10, 11] confirms the structural sensitivity of these features, as corroborated by theoretical calculations using either the multiple scattering XANES type approach or the locally projected density of states. Consequently it seems reasonable in the present study to attribute the reference TiO_2-O K edge in the interface A case to anatase and its equivalent in the interface B case to a "disordered" rutile structure. We introduce this distinction because the three peaks which should occur in the rutile case are not well resolved in the present case but constitute a broad band, suggesting some disorder on the second and higher neighbour arrangement.

In order to further analyse the modification of the O-K edge across the line spectrum sequence, every experimental spectrum is then fitted with a linear combination of the two reference spectra (TiO_2 and SiO_2) extracted from the same sequence. It offers the extra advantage that all spectra are recorded in exactly the same experimental conditions, reducing then the source of bias effects which could be instrumentally introduced.

A multiple least square (MLS) fit decomposition of the O K edge after background subtraction, on the window 526-550 eV, is then used to determine the weight of each reference in any spectrum of the sequence; the quality of the fit is indicated by its χ^2 value. The results are shown in Figure 6. In both cases, the presence of the interface is clearly visible, its location being defined by the spectrum number for which the weight of each component is approximately equal to 0.5; the width of the interfacial zone can also be estimated as the distance between the spectrum where 80% of the signal is due to O K-SiO_2 and the spectrum where 80% of the signal is due to O K-TiO_2. It appears that interface A is rather narrow ($\approx$ 3.5 nm) and symmetrical, while interface B is wider ($\approx$ 8 nm) and asymmetrical (it is larger on the SiO_2 side than on the TiO_2 one). Of course these widths include the broadening due to the width of the incident probe, nominally of the order of 0.7 nm in the present configuration, and to the lateral spreading of the beam when propagating through the specimen. As a consequence of the change in local thickness between the analysed areas, this broadening effect should be much more pronounced on interface A than on interface B. Therefore the "chemical width" (width of the interfacial zone as defined above) is much smaller on interface A than on interface B.

For both interfaces, the χ^2 values are higher on the TiO_2 side, which can be due to the fact that background removing under the O K edge is made more difficult by the presence of strong oscillations due to Ti $L_{2,3}$ edge fine structures. It has several consequences. As the fitting procedure implies the comparison between the experimental spectrum acquired for a given probe position and the reference spectrum averaged over several probe positions far from the interface, without intensity scaling factor, it is not surprising to observe values of the weighting factor scattered around the value 1 on the TiO_2 side. The fluctuations of the order of $\pm 10\%$ can likely be attributed to the difficulties of modelling the background, before subtraction of the characteristic O K edge, over an energy window corresponding to the oscillating fine structures on the Ti $L_{2,3}$ high energy tail.

As for the evaluation of the uncertainties on the model weight determination, it must be pointed out that they are due both to statistical and systematic sources. For the first ones, the knowledge of the noise and gain fluctuations in each energy loss channel of the parallel detector is required, and this procedure has not been applied during the present study. For the second ones, as mentioned above, they are too much dependent on difficulties associated with background modelling. Consequently it is not possible in the present state to provide reliable error bars. But the fact that at both extremities of the scan the weight factors seem to stabilize respectively around the expected values of 0 and 1 constitutes a satisfactory proof that the uncertainties remain limited at most between $\pm 10\%$.

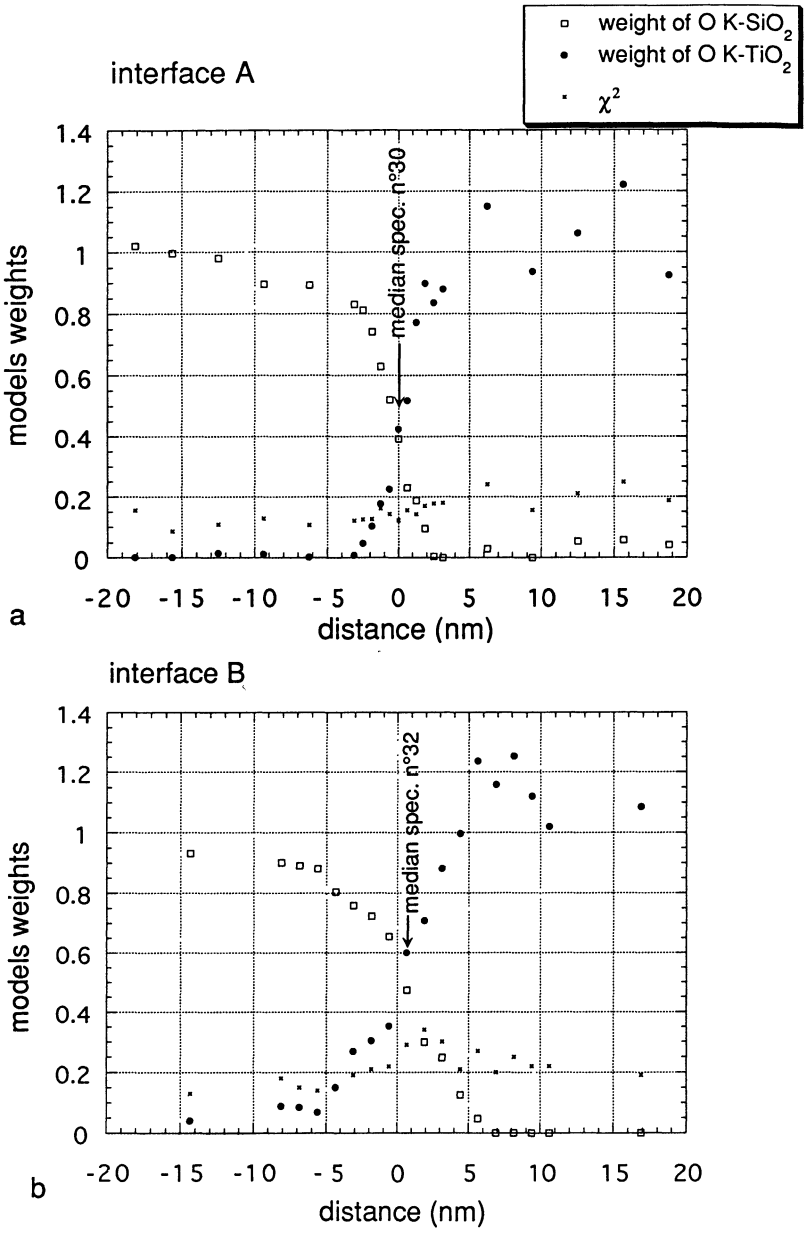

Fig. 6. — Weights of reference spectra O K edge in SiO_2 and in TiO_2 as defined in Figure 5 determined by MLS decomposition: a) for interface A, b) for interface B. Reduced χ^2 is also figured with arbitrary units.

Furthermore, one observes a slightly higher χ^2 value in the neighbourhood of interface B than of interface A. In order to evaluate the quality of the fit and the existence of eventual discrepancies, we have compared the experimental median spectrum in each sequence with the reconstructed equivalent one (Fig. 7). For interface A (spectrum n°30) the agreement is quite satisfactory over the whole energy loss range; the splitting of the O K prepeak is equivalent in both experimental

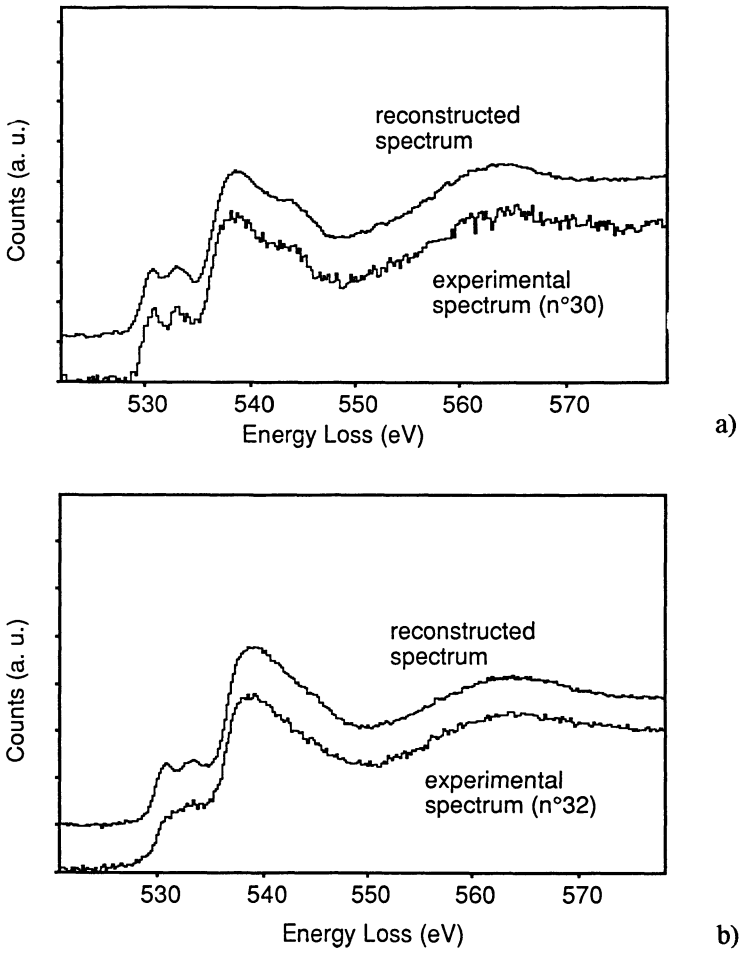

Fig. 7. — Comparison between experimental and reconstructed O K edge for median spectra: a) interface A, b) interface B. Note that the prepeak is not split into two lines for interface B.

and reconstructed spectra. But for interface B the prepeak of the experimental median spectrum (n°32) is not split, while the reconstructed one exhibits a splitting according to the shape of the reference spectrum.

This comparison further confirms that artefacts due to thickness dependent multiple scattering events can be ruled out. They would modify the fit dominantly around 25 eV above threshold (average value of the plasmon peak both in SiO_2 and TiO_2). The observed discrepancies between experimental and reconstructed spectra concern only a narrow energy range fit above threshold, while the fit seems always satisfactory at higher energy losses ($\approx 15 - 25$ eV) above threshold.

Similarly to the discussion of errors along the intensity scale in Figure 6, what can be said about errors along the position scale in the same figure? One can question how far the specimen drift can modify the scale. The basic parameter to be considered is the ratio between an eventual drift (or more important its projection along the axis normal to the interface) during the spectrum acquisition at a given pixel and the increment step between two successive measurements. To evaluate this factor, we have compared lower magnification images (either BF or ADF) before

and after the line-spectrum acquisition. When the scan can be visualized by contamination or irradiation tracks (which does not happen in any cases), it has been possible to estimate an upper value for this drift of the order of 0.01 to 0.02 nm/s, so that the errors on the distance axis is at maximum of the order of 15%.

4. Discussion of the Fine Structures Analysis

ACROSS THE INTERFACE. — The above quantitative analysis of fine structures changes only deals with the oxygen K edge. It defines the mean position of the interfaces as that corresponding to the median spectrum (equal number of oxygen atoms with Ti environment similar to TiO_2 and with Si environment similar to SiO_2). It also discriminates the interfaces in terms of "chemical width". How far can we proceed further in the analysis and connect these behaviours to different types of interfaces?

Generally speaking, it is possible to identify two major classes of interfaces. In the first case, the interface between the two materials is abrupt, but roughness can be present as a consequence of the non-planarity of the interfaces. In this situation, the energy loss spectrum measured for any position across the interface corresponds to the relative proportion of each material along the trajectory of the beam across the specimen thin foil, and can then be modelled as a linear combination of the two reference spectra. In the second case, the interface between the two materials is smooth but an interfacial region is formed due to the interdiffusion of atoms between the materials. In this latter case, it should be possible to identify in the neighbourhood of the interface some EELS fine structures which cannot be fitted to a combination of reference spectra, but are representative of hybrid environments, such as Si-O-Ti in the present study.

Consequently, we have displayed in Figures 8a and 8b the sequences of spectra corresponding only to the neighbourhood of both interfaces in order to correlate the detailed changes observed on the oxygen prepeak to those occurring on the Ti $L_{2,3}$ edge. Several criteria can be proposed to estimate quantitatively these changes as the probe is scanned across the interface from the SiO_2 to the TiO_2 side. The first one is the plot of the number of Ti atoms, defined on the intensity of the Ti $L_{2,3}$ edge after background subtraction (see hatched area in Fig. 4). This can be considered as the reference atomic point of view from the Ti side and the curves relative to the investigated interfaces are shown in Figure 9. The second criterion is the plot of the oxygen prepeak as defined in Figure 4. In practice, we have subtracted for each spectrum a scaled curve corresponding to the low energy tail of the O K edge in SiO_2. The resulting plots are also shown in Figure 9, to be compared with the previous ones. The two interfaces exhibit clear differences: in the first one (interface A), the decrease of both signals connected to the presence of Ti atoms and to the existence of Ti-O octahedral environments are well correlated within one probe step. In the second one (interface B), the decrease of the weight of the Ti-O antibonding orbital is faster than the decrease of the number of Ti atoms, suggesting therefore the existence of some mixed TiO_2-SiO_2 solid solution with Si-O-Ti bonds [12] in a zone of about 5 nm width. A final criterion is the visibility of the crystal-field splitting on both Ti L lines and O K prepeak, which is representative of the quality of the local crystal symmetry. It is difficult to propose a quantitative measurement for this effect. The only easy observation is that this splitting appears much faster in the case of interface A than for interface B. The absence of splitting has already been reported as well for amorphous, *i.e.* disordered, TiO_2 [13] as for substoichiometric TiO_x. However in the latter case a shift of the Ti $L_{2,3}$ edge should be observed [14]. In the present study, no detectable shift has been found in the neighbourhood of the interface, confirming the hypothesis of the existence of a TiO_2-SiO_2 solid solution. It is also interesting to notice that the appearance of the XANES-type oscillations on the high energy side of the Ti L edge (labelled peaks B, C and D in Fig. 4) follows that of the splitting, corroborating the description in terms of loss of local crystal symmetry.

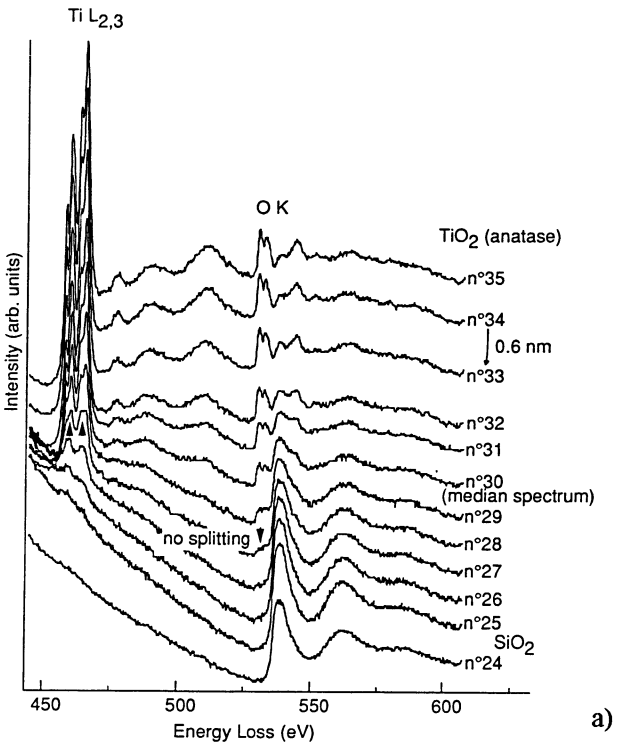

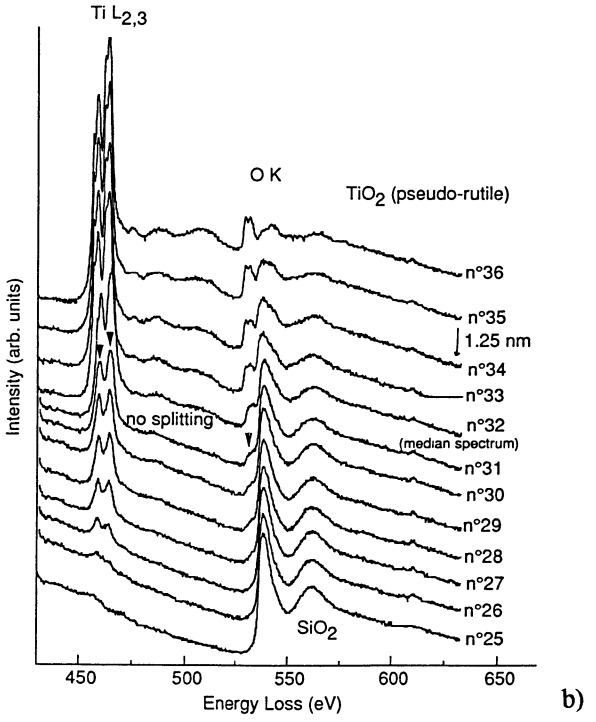

Fig. 8. — Series of individual spectra in the interfacial zone: a) interface A, b) interface B.

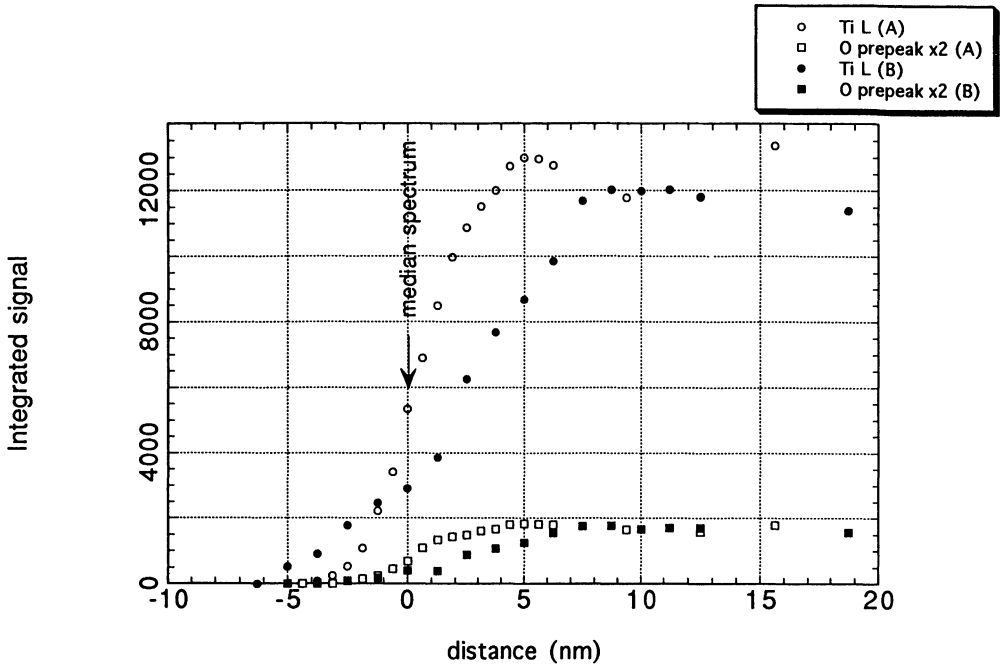

Fig. 9. — Intensity of Ti $L_{2,3}$ and O K prepeak signals. The background has been subtracted by a power law and the contribution of O K-SiO_2 removed. In the first interface (A), the decrease of both signals connected to the presence of Ti atoms and to the existence of Ti-O octahedral environments are well correlated within one probe step. In the second one (interface B), the decrease of the weight of the Ti-O antibonding orbital is faster than the decrease of the number of Ti atoms. In particular, the Ti L signal comes to 0 at a distance of 6 nm with respect to the medium spectrum while the O prepeak signal reaches zero over 2 nm. On the TiO_2 side in both cases the ratio between the Ti and the O prepeak signal remains rather stable.

The differences observed between the two interfaces can then reasonably be explained in terms of the differences in microstructures when TiO_2 is evaporated on a thermal SiO_2 layer and on evaporated SiO_2 layer. Thermal SiO_2 is a compact material with density very close to the one of fused silica (*i.e.* ≈ 2.2 g/cm^3). The microstructure of SiO_2 evaporated films depends strongly on the deposition parameters: substrate temperature T_S, pressure in the chamber (base pressure or O_2 partial pressure), deposition speed v. In our conditions, $T_S = 250$ °C, $P_{O_2} = 1.5 \times 10^4$ Torr, $v \approx 0.5$ nm/s; the pore volume fraction is about 0.2, leading typically to a density of 2.1 g/cm^3. The higher porosity of evaporated SiO_2 offers therefore an increased surface for chemical reactivity with TiO_2. It could explain the enhanced interdiffusion and increased chemical width observed in the present experiment for interface B as compared with interface A.

Radiation Damage Effects. — At the end of the spectrum-line A, the last few spectra also exhibit changes in fine structure (Fig. 10). The first phenomenon is the global decay of both Ti $L_{2,3}$ and O K signals, suggesting a partial mass loss induced by radiation damage. Simultaneously, one notices the disappearance of the splitting on Ti $L_{2,3}$ and O K edges, as well as the decay of the extended fine structure of Ti $L_{2,3}$ edge. As no shift on the Ti L_3 edge position is observed, contrary to the case investigated in reference [14] where this shift was explained by a reduction of TiO_2 down

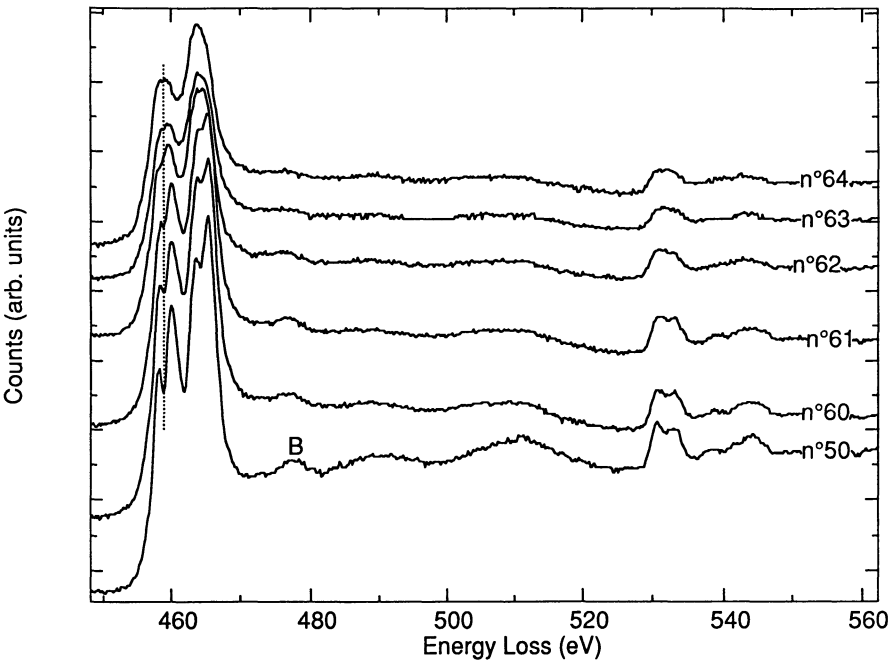

Fig. 10. — Five last spectra of the spectrum-line A. Spectrum n°50 is presented as a reference. Note that the "crystal field" splitting gradually disappears.

to TiO, it is likely that the damage observed in the present work only involves an amorphization process. As a matter of fact, Rez *et al.* have used a dose (10 nA in a 10 nm nanometer probe during 200 s, corresponding to about 2×10^{11} electrons/nm^2) 10 times more intense than in our work (0.2 nA in a 0.7 nm diameter probe during 8 s, about 3×10^{10} electrons/nm^2).

In a further step, it would be necessary to investigate, within the relevant range of electron doses, how the different materials behave as a function of local thickness. Such data would be required to eliminate the uncertainties in the present analysis related to the weight of beam induced chemical changes at the interface as compared to growth-induced chemical changes.

5. Conclusions

This study has demonstrated the high capabilities of EELS for investigating at the ultimate level the local chemistry and the electronic structures in the immediate vicinity of the interface between two dielectric materials. New fitting procedures, employing reference spectra acquired during the same line-spectrum sequences, on the bulk material on both sides of the interface, have been used. A quantitative analysis of the changes in different fine structures on the titanium and oxygen edges enables to clearly discriminate different levels of interdiffusion at the boundary.

Acknowledgements

We wish to thank M. Tencé (LPS, Orsay) for developing all customs functions that enable spectrum-line acquisition and subsequent data processing.

References

[1] Yu-Zhang K., Boisjolly G., Rivory J., Kilian L. and Colliex C., *Thin Solid Films* **253** (1994) 299-302.

[2] Colliex C., Tencé M., Lefèvre E., Mory C., Gu H., Bouchet D. and Jeanguillaume C., *Mikrochim. Acta* **114/115** (1994) 71-87.

[3] Lotiaux M., Boulesteix C., Nihoul G., Varnier F., Flory F., Galindo R. and Pelletier E., *Thin Solid Films* **170** (1989) 107-115.

[4] Lucovsky G., Manitini M.J., Srivastava J.K. and Irene E.A., *J. Vac. Sci. Technol.* **B5** (1987) 530-537.

[5] Theil J.A., Tsu D.V., Watkins M.W., Kim S.S. and Lucovsky G., *J. Vac. Sci. Technol.* **A8** (1990) 1374-1381.

[6] Wang Y., to be published.

[7] Wang Y., Thèse, Université Paris VI (1995).

[8] de Groot F.M.F., Grioni M., Fuggle J.C., Ghijsen J., Sawatzky G.A. and Petersen H., *Phys. Rev. B* **40** (1989) 5715-5723.

[9] Kurata H., Lefevre E., Colliex C. and Brydson R., *Phys. Rev. B* **47** (1993) 13763-13768.

[10] Brydson R., Williams B.G., Engel W., Sauer H., Zeitler E. and Thomas J.M., *Solid State Commun.* **64** (1987) 609-612.

[11] Brydson R., Sauer H., Engel W., Thomas J.M., Zeitler E., Kosugi N. and Kuroda H., *J. Phys.: Condens. Matter* **1** (1989) 797-812.

[12] Stakheev A.Yu., Shpiro E.S. and Apijok J., *J. Phys. Chem.* **97** (1993) 5668-5672.

[13] Manoubi T., Thèse, Université Paris XI (1989).

[14] Rez P., Weiss J.K., Medlin D.L. and Howitt D.G., *Microsc. Microstruct. Microanal.* **6** (1995) 433-440.